4404 *J. Phys. Chem. A* **2005,** *109,* 4404−4409

Intramolecular Dynamics of 1,2,3-Trifluorobenzene Radical Anions As Studied by OD ESR and Quantum-Chemical Methods

Maria M. Barlukova,[†,‡] **Irina V. Beregovaya,**[§] **Victor P. Vysotsky,**[§] **Lyudmila N. Shchegoleva,***[,§] **Victor A. Bagryansky,**[†,‡] **and Yuri N. Molin**[†]

Institute of Chemical Kinetics and Combustion, 630090 Novosibirsk, Russia, Novosibirsk State University, 630090 Novosibirsk, Russia, and N. N. Vorozhtzov Novosibirsk Institute of Organic Chemistry, 630090 Novosibirsk, Russia

Received: February 8, 2005; In Final Form: April 1, 2005

Ab initio UMP2, RMP2, DFT/UB3LYP, and CBS-QB3 calculations have shown that the adiabatic potential energy surface (PES) of the 1,2,3-trifluorobenzene radical anion is a pseudorotation surface formed by nonplanar stationary structures. The low (∼2−4 kcal/mol) energy barriers in the path of pseudorotation imply manifestations of spectral exchange in the ESR spectra of this radical anion. The optically detected ESR of radical ion pairs was used to obtain the ESR spectrum of 1,2,3-trifluorobenzene radical anion in liquid squalane solution and to study temperature variations in the spectrum over the range of 243−325 K. The spectrum is a doublet of triplets with hfc constants of $a_{F(2)} = 29$ mT and $a_{2F(1,3)} = 7.6$ mT at T = 243 K. The experimental hfc constants are temperature-dependent. Calculations of the temperature dependence of hfc constants in the framework of the model of classical nuclei motion along the pseudorotation coordinate reproduce well the experimental data.

1. Introduction

The radical ions of fluorine-substituted benzenes were the objects of numerous experimental and theoretical investigations (e.g., refs 1−4 and references herein). The interest in these ions is due to the peculiarities of their electron and spatial structures. The high values of hfc constants of the radical anions of fluorine-containing benzene derivatives testify to the disturbance of their planar structure due to the pseudo-Jahn−Teller effect.[1] The out-of-plane distortions are caused by a strong perturbation of the benzene σ-system by fluorine atoms, which generates the low-lying excited σ-states of radical anion.

With respect to the benzene π-system, fluorine is a weakly perturbing substituent. In the low-symmetry (D_{2h}, C_{2v}) molecules of partially fluorinated benzenes, the energy splitting of the boundary π-MO levels, degenerate in benzene, is rather small (see, e.g., the data of photoelectron and electron capture spectroscopy[2]). Therefore, for their radical ions there are two close in energy π-states whose terms can cross.

As shown recently,[5,6] at the Hartree−Fock (HF) level of calculations, the crossing of π state terms occurs for both the radical anions and cations of most of the fluorobenzenes. Thus, on the potential energy surface there are two stationary π radical structures differing in symmetry of the ground electron state ($^2B_1$ and $^2A_2$ in terms of the C_{2v} group). As a result of avoided crossing of the π state terms, the HF PESs of the radical ions of low-symmetry partially fluorinated benzenes preserve the form of pseudorotation surface that is peculiar to the Jahn−Teller benzene radical ions. For radical anions, the PES structure is complicated by the existence of mirror-symmetric nonplanar structures.[5]

Among the fluorinated benzenes ions, the 1,2,3-trifluorobenzene (TFB) radical ions possess the minimum energy splitting of the π structure levels. The recent nonempirical calculations show that for the TFB$^{\bullet+}$ radical cation the pseudorotation is also preserved at the post-HF level of calculations.[6,7] As compared with HF calculations, in this case, the height of the energy barriers for pseudorotation decreases. This paper reports an ab initio study of the adiabatic PES of the TFB$^{\bullet-}$ radical anion by MP2 and DFT/B3LYP methods. The results obtained show that the anion PES also retains the form of pseudorotation surface with low (∼2−4 kcal/mol) energy barriers that separate local minima. The pseudorotation gutter is formed by nonplanar radical anion structures.

The structure distortions and thermal transitions among various geometrical configurations of TFB radical ions should lead to hyperfine interaction modulation revealed in ESR spectra as a spectral exchange. In this case, the ESR spectrum should depend on temperature. We failed to find published ESR spectroscopy data on TFB radical ions. So far, the temperature dependence of the ESR spectra of benzene fluorine derivatives radical ions has not been studied.

One of the main obstacles to the ESR study of fluorine-substituted benzene radical ions is the instability of these particles. Because the concentration required for conventional ESR is sufficiently high (>10^{11} spins per sample), ESR spectra of these short-lived particles can be obtained only under special conditions (as a rule, frozen solutions at low temperatures). At the same time, the optically detected ESR (OD ESR) method, being highly sensitive for radical ion pairs, can register them even at very low concentrations (>10^4 spins per sample).[8]

In the present work, the OD ESR method was used to record the ESR spectrum of the 1,2,3-trifluorobenzene radical anion in liquid squalane solution and to measure its temperature

---

* Corresponding author. Tel: +7 3833 306 859. Fax: +7 3833 309 752. E-mail: sln@quant.nioch.nsc.ru.

[†] Institute of Chemical Kinetics and Combustion.

[‡] Novosibirsk State University.

[§] N. N. Vorozhtzov Novosibirsk Institute of Organic Chemistry.

10.1021/jp050683a CCC: $30.25

TABLE 1: Stationary PES Structures of the 1,2,3-Trifluorobenzene Radical Anion[a]

calculation method	structure	$E_{\rm tot}$	N^b	$\langle S^2 \rangle$	$E_{\rm rel,}$	$E_{\rm rel}^{\rm ZPE}$
ROHF/6-31+G*[5]	C_s	−527.204096	0		0.93	0.92
	C_1(A)	−527.198222	1		4.62	3.62
	C_1(B)	−527.205581	0		0	0
	C_2	−527.195525	1		6.31	5.19
UMP2/6-31+G*	C_s	−528.502015	0	0.896	1.92	
	C_1(A)	−528.501242	1	0.892	2.41	
	C_1(B)	−528.505075	0	0.821	0	
	C_2	−528.498153	1	0.857	4.34	
PUMP2/6-31+G*//UMP2/6-31+G*	C_s	−528.511886		0.765	0	
	C_1(A)	−528.510788		0.763	0.69	
	C_1(B)	−528.510609		0.752	0.80	
	C_2	−528.506006		0.755	3.69	
RMP2/6-31+G*	C_s	−528.556354			0	
	C_1(A)	−528.550305			3.80	
	C_1(B)	−528.550590			3.62	
	C_2	−528.549831			4.09	
UB3LYP/6-31+G*	C_s	−529.709613	0	0.759	0	0
	C_1(A)	−529.705929	1	0.763	2.31	1.81
	C_1(B)	−529.706811	0	0.759	1.76	1.68
	C_2	−529.703361	1	0.759	3.92	3.13
UB3LYP[c]/aug-cc-pVDZ	C_s	−530.003792	0	0.761	0	0
	C_1(A)	−530.000127	1	0.762	2.30	1.83
	C_1(B)	−530.000849	0	0.759	1.85	1.76
	C_2	−529.997942	1	0.758	3.67	2.90
CBS-QB3	C_s	−529.335392	0		0	0
	C_1(A)	−529.331702	1		2.32	1.74
	C_1(B)	−529.332841	0		1.60	1.55
	C_2	−529.330420	1		3.12	2.32

[a] The total energies are given in atomic units (au), and the relative ones, in kcal/mol. [b] Number of imaginary vibration frequencies. [c] Here the GAUSSIAN B3LYP functional is used.

dependence. Experimental results are compared with the predictions of quantum-chemical calculations of hfc constants and the PES shape.

2. Methods

2.1. Computational Details. The geometry of stationary TFB$^{\bullet-}$ structures was optimized at the MP2/6-31+G* level of calculations (UMP2-frozen core and RMP2-full). Besides, we performed UB3LYP calculations using basis sets 6-31+G* and aug-cc-pVDZ. To estimate the relative energies of stationary structures, we also used the combined calculation technique CBS-QB3.[9]

According to the calculations, the TFB molecule displays a negative electron affinity in gas phase. Therefore, it is worth noting that the anion states considered below are bonded states, which is confirmed by special stabilization calculations.[5]

The types of stationary PES points were determined by normal vibration analysis. Interrelations between the points were established by intrinsic reaction coordinate (IRC) calculations. For zero point vibrations energies (ZPVE) we used the scale factors 0.9135 and 0.9806 for ROHF and B3LYP calculations, respectively.[10]

The UMP2 calculations of stationary structures were supplemented with the annihilation of a quartet component (PUMP2/6-31+G*//UMP2/6-31+G*). The hfc constants were calculated by the UB3LYP method with the 6-31+G*, aug-cc-pVDZ, and EPRIII basis sets. In our calculations, we used the program packages GAMESS,[11] GAUSSIAN-94,[12] and CADPAC.[13] The structure images and SOMO plots were made by the MOLDEN program.[14]

2.2. Experimental Details. The OD ESR method[15,16] was used to detect the spin-correlated radical ion pairs forming in diluted solutions of TFB and *p*-terphenyl-d_{14} under ionizing radiation. The value to be measured is the dependence of the recombination fluorescence intensity of solution on the strength of the static magnetic field under the action of a microwave field. In the case of low microwave power, the OD ESR spectrum is the superposition of the ESR spectra of both of the recombining radical ions of the same integral intensity.[15]

The measurements were performed using an OD ESR spectrometer based on an ER-200D Bruker ESR-spectrometer[8] equipped with a source of ionizing radiation (an X-ray tube) and a photomultiplier to measure the fluorescence intensity. The OD ESR spectra were recorded with a microwave power of 5 W and a modulation amplitude of 0.9 mT. To determine hfc constants, the recorded OD ESR spectra were simulated using the “WinSim-2002” program.[17]

1,2,3-Trifluorobenzene (99%, ABCR) and *p*-terphenyl-d_{14} (*p*-TP) (99%, Aldrich) were used as received.

Squalane (2,6,10,15,19,23-hexamethyltetracosane, 99%, purchased from Fluka) was purified on a chromatographic column with alumina activated with silver nitrate (10%). The solvent purity was monitored by its UV absorption spectrum. The optical density of the fraction used was 1 at a wavelength of 210 nm in a 1 cm layer. Solutions were degassed by repeated freeze−pump−thaw cycles.

3. Results and Discussion

The total and relative energies of stationary PES structures of the TFB$^{\bullet-}$ radical anion are summarized in Table 1 and compared with results of ROHF/6-31+G* calculations.[5] All the calculations reveal the four types of stationary structures on PES (Figure 1): two minima (structures C_s and C_1(B)) and two saddle points (structures C_2 and C_1(A)), which are the transition states for pseudorotation. The complete scheme of pseudorotation in TFB$^{\bullet-}$ is shown in Figure 2. It almost reproduces the pseudorotation scheme for the hexafluorobenzene radical anion.[18] The only difference is that the TFB$^{\bullet-}$ PES minima (and transition states) are energetically nonequivalent. When calculations of

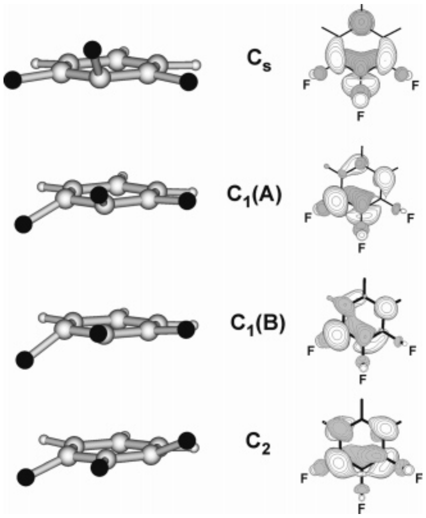

Figure 1. Stationary structures on the PES of the 1,2,3-trifluorobenzene radical anion and their SOMO plots.

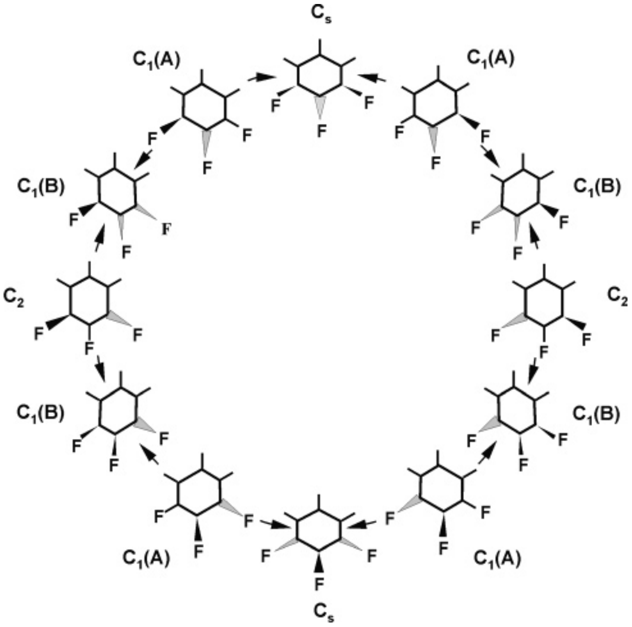

Figure 2. Pseudorotation scheme of the 1,2,3-trifluorobenzene radical anion.

TABLE 2: Calculated ^{19}F hfc Constants a_F for Stationary Structures of the 1,2,3-Triflouorobenzene Radical Anion (UB3LYP)[a]

		structure			
basis set	^{19}F nuclei	C_s	C_1(A)	C_1(B)	C_2
6-31+G*	F_1	8.33	20.49	25.55	16.51
	F_2	30.29	20.66	12.38	16.20
	F_3	8.33	9.18	6.31	16.51
aug-cc-pVDZ	F_1	7.54	19.39	24.54	15.46
	F_2	29.43	19.91	11.45	14.66
	F_3	7.54	8.40	5.74	15.46
EPRIII	F_1	8.40	21.43	26.71	17.13
	F_2	31.92	21.73	12.94	16.56
	F_3	8.40	9.19	6.37	17.13

[a] hfc constants are given in units of mT.

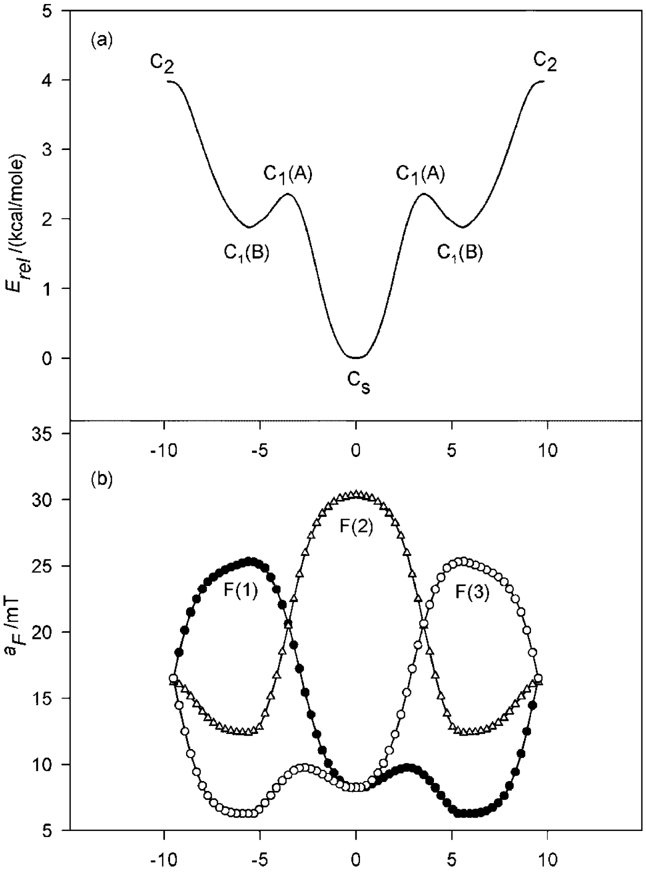

Figure 3. Changes in energy (a) and in ^{19}F hfc constants (b) of the 1,2,3-trifluorobenzene radical anion during the motion along the pseudorotation coordinate from the C_2 transition states to C_s minima (UB3LYP/6-31+G*).

higher level than the HF ones are used, the barrier height in the path of pseudorotation decreases.

At the HF calculation level, the global PES minimum corresponds to the asymmetric C_1(B) structure. However, taking into account electron correlation, the C_s structure starts to display a lower energy. The UMP2 method is an exception due to the different degrees of spin contamination of a wave function for various stationary structures of the radical anion (Table. 1). Annihilation of the quartet component admixture in the wave function (PUMP2) leads to stabilization of a more symmetric C_s structure.

Thus, all the methods we used predict the same form of pseudorotation pathway. There are no great differences in the quantitative estimation of barrier heights (~2−4 kcal/mol). This result points out a structural flexibility of the TFB$^{•-}$ radical anion with respect to the pseudorotation coordinate.

The ^{19}F hfc constants, a_F, calculated by the UB3LYP method for stationary structures of TFB$^{•-}$ are summarized in Table 2. For all the basis sets used, the hfc constants with ^{1}H nuclei do not exceed 0.59 mT and cannot be observed by the OD ESR method under our experimental conditions. The results obtained by different basis sets are close and demonstrate a substantial redistribution of the unpaired electron density during pseudorotation, which is due to a change in the electron state and structure of radical anion. The changes in a_F values along the minimum energy path from the C_2 transition state to the global C_s minimum according to the UB3LYP/6-31+G* IRC calculation are shown together with a corresponding energy profile in Figure 3. It is worth noting that the energy as well as the $a_{F(2)}$ value vary in the same way when passing in both directions from the global C_s minimum. At the same time, the plots of $a_{F(1)}$ and $a_{F(3)}$ vs pseudorotation coordinate are the mirror reflection of each other. It is concluded then that in the case of fast exchange, the F(1) and F(3) nuclei will be magnetically equivalent, the

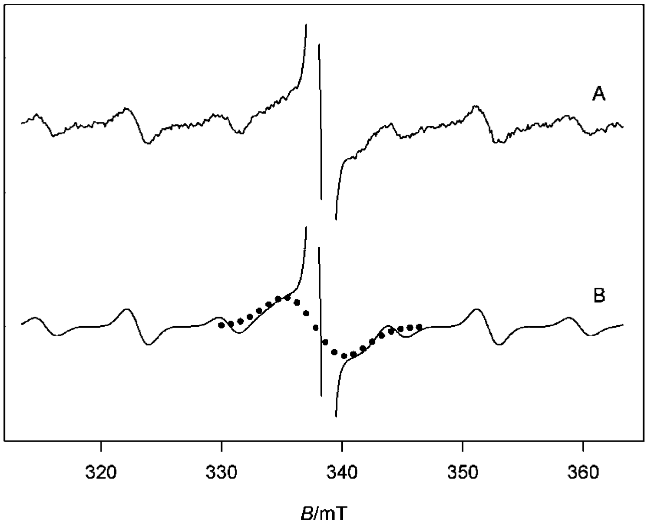

Figure 4. OD ESR spectrum of the 1.5×10^{-3} M *p*-TP + 10^{-2} M TFB solution in squalane at $T = 243$ K (A) and the spectrum simulation (B) with parameters $a_{F(2)} = 29$ mT and $a_{2F(1,3)} = 7.6$ mT for $TFB^{\bullet-}$. The width of the unresolved signal is 2.45 mT for TFB RC; there is no hfc for $p\text{-}TP^{\bullet+}$ and $p\text{-}TP^{\bullet-}$. The circles denote the simulation of the signal of the TFB radical cation.

hfc constant $a_{2F(1,3)}$ being equal to the averaged value of $a_{F(1)}$ and $a_{F(3)}$.

To record the OD ESR spectra of a radical ion pair, at least one of the pair partners should yield, after pair recombination, an excited molecule with a high quantum yield of fluorescence. Therefore, a luminophore, which is a hole acceptor and forms a pair with the TFB radical anion should be added to the solution. In this case, as luminophore we used *p*-TP with a fluorescence quantum yield close to unity and capable of trapping both electron and solvent hole (ionization energy IE = 7.83 eV[19] and electron affinity EA = 0.51 eV[20]).

The ionization potential (IE) of TFB is 9.4 eV,[21] which is below the values typical of alkanes. The experimental electron affinity value of TFB is unavailable. According to our calculations, in the gas phase, EA ~ -0.3 eV. It is known, however, that the other fluorine-substituted benzenes capture electrons in a nonpolar solvent.[22] It is assumed then that in a squalane solution, TFB will capture both positive and negative charge to form pairs with *p*-TP radical anions and cations. Special experiments revealed an absence of OD ESR signal in squalane solution of TFB probably as a result of low quantum yield of TFB fluorescence.

In our experiment, we used squalane solutions containing 1.5×10^{-3} M *p*-TP and 10^{-2} M TFB. The OD ESR spectrum of such a solution (Figure 4) results from the superposition of the *p*-TP and TFB radical ions spectra. Because the four types of pairs can be formed: $TFB^{\bullet+}/TFB^{\bullet-}$, $p\text{-}TP^{\bullet+}/p\text{-}TP^{\bullet-}$, $p\text{-}TP^{\bullet+}/TFB^{\bullet-}$, and $TFB^{\bullet+}/p\text{-}TP^{\bullet-}$, the spectrum can exhibit the lines of all four particles. The central single line in the spectrum belongs to the *p*-TP radical anions and cations. In addition, there are a doublet of triplets relevant to the TFB radical anion (the hfc constants at $T = 243$ K are $a_{F(2)} = 29$ mT and $a_{2F(1,3)} = 7.6$ mT) and a wide unresolved signal at the center belonging, probably, to the TFB radical cation. That the multiplet lines are associated with the TFB radical anion is confirmed by the fact that the splitting values in the multiplet are close to the calculated values of hfc constants for the most energetically advantageous C_s structure of the radical anion (Table 2). At the same time, the width of the unresolved signal equal to 2.45 mT is close to a value of 2.25 mT obtained from hfc constants calculated by the UB3LYP/6-31G* method for the minimum energy structure of the TFB radical cation ($C_{2v}(^2B_1)$):[6,7] $a_{F(2)} = 4.37$ mT, $a_{2F(1,3)} = 0.85$ mT, $a_{2H(4,6)} = -0.01$ mT, and $a_{H(5)} = -0.92$ mT.

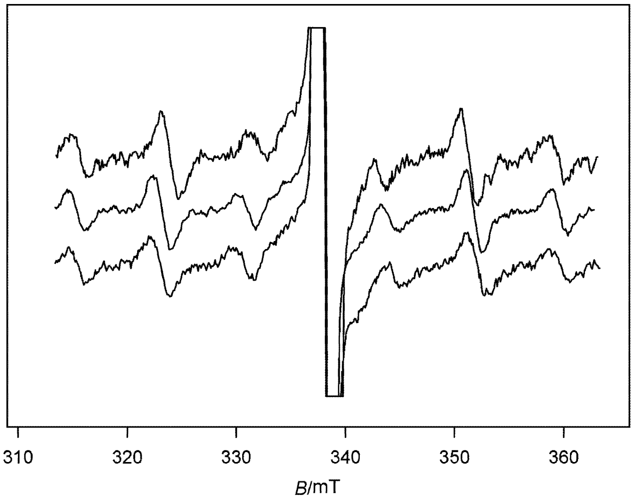

Figure 5. OD ESR spectrum of the 1.5×10^{-3} M *p*-TP + 10^{-2} M TFB solution in squalane at temperatures (from bottom to top) 243, 259, and 309 K.

Figure 5 shows the OD ESR spectra of the 1.5×10^{-3} M *p*-TP + 10^{-2} M TFB solution for various temperatures. The lines of the TFB radical anion shift with increasing temperature to the center of the spectrum. In this case, the shift of central lines is stronger than that of the outermost ones whereas the width of each line remains unchanged. These peculiarities are typical of the fast spectral exchange wherein each magnetic nucleus is characterized by the hfc constant that is average over the available conformations.[23] For low temperatures, the states close to the energy minimum (the C_s structure) are mainly populated and the observed hfc constants are close to those calculated for this minimum. As the temperature increases, the contribution of the states of higher energy also increases, which leads to the shift of lines in the spectrum. The assumption of fast exchange is in agreement with the predicted low energy barrier between the C_s and C_1(B) structures.

The temperature variations, observed in the spectrum, were interpreted using results of the UB3LYP/6-31+G* IRC calculations (Figure 3). The temperature dependence of hfc constants was considered in the model of fast exchange between conformations lying along the pseudorotation coordinate Q. The averaged values of hfc constants, a_{av}, were calculated from the classical Boltzmann distribution

$$a_{av} = \frac{\int e^{-E(Q)/kT} a(Q)\, dQ}{\int e^{-E(Q)/kT}\, dQ} \tag{1}$$

Figure 6 presents the results of calculations performed with eq 1 together with the hfc constants determined experimentally for various temperatures. As follows from Figure 6, at all temperatures, the calculated hfc constants exceed somehow the experimental ones. A relative excess is 3% for $a_{F(2)}$ and about 15% for $a_{2F(1,3)}$. However, for both of the constants, these calculations reproduce the linear character and slope of the temperature dependences over the range under study. This shows that the form of the pseudorotation gutter was predicted correctly.

It is worth noting that the use of eq 1 is based on the following assumptions.

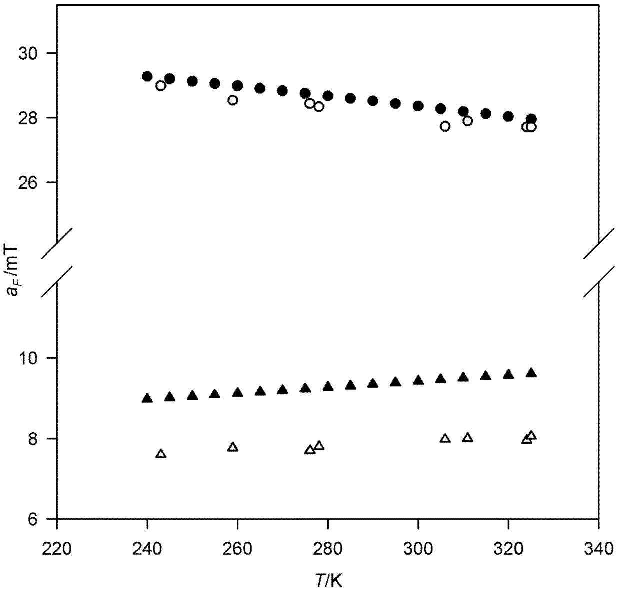

Figure 6. Temperature dependence of the experimentally measured hfc constants $a_{F(2)}$ (open circles) and $a_{2F(1,3)}$ (open triangles) and the results of the calculations of this dependence in the framework of the classical model (black circles and triangles) with hfc constants and energy given in Figure 3.

(i) There is a relatively weak change of hfc constants at the shift of nuclei along the low-frequency modes differing from the pseudorotation one. It is confirmed by the fact that as compared with pseudorotation, much higher barriers should be overcome for substantial redistribution of the unpaired spin density moving along the other modes. Besides, we estimated the changes in hfc constants for the C_s and C_1(B) structures upon the nuclei shift along the coordinate of the most low-frequency vibration (Table 3) corresponding to a ∼kT increase in energy.

The calculations were made with the program Normal.[24] In both cases, the changes obtained do not exceed 0.5 mT, the general tendency of hfc constants change when passing from the C_s to C_1(B) structure (a decrease of a_F and an increase of a_{2F}) being preserved.

All other normal vibrations have higher frequencies (more than 200 cm^{-1}) and thus smaller amplitudes of thermal vibrations. It is assumed then that their contribution to the change in hfc constants will be even smaller.

(ii) The nuclei motion along other coordinates does not lead to various statistical weights of points in the path of pseudorotation. To discuss this assumption, let us use vector $\mathbf{Q}'$ to denote the set of all normal coordinates except the pseudorotation coordinate Q. Thus, in the framework of assumption (i), the average hfc constant can be written as

$$a_{av} = \frac{\int e^{-E(Q,\mathbf{Q}')/kT} a(Q)\, dQ\, d\mathbf{Q}'}{\int e^{-E(Q,\mathbf{Q}')/kT}\, dQ\, d\mathbf{Q}'} = \frac{\int e^{-E(Q,0)/kT} a(Q)\, \rho(Q)\, dQ}{Z} \qquad (2)$$

where $E(Q,0)$ is the value of energy at point Q in the path of pseudorotation, Z is the partition function, and the statistical weight $\rho(Q)$ of this point,

$$\rho(Q) = \int e^{-(E(Q,\mathbf{Q}')-E(Q,0))/kT}\, d\mathbf{Q}' \qquad (3)$$

is the incomplete partition function calculated over all coordinates except Q for a fixed value of the latter. As follows from eqs 1 and 2, more rigorous averaging (2) converts into (1) if the statistical weight $\rho(Q)$ is weakly dependent on the coordinate Q. To verify this condition, we calculated the incomplete partition function for each structure: C_s, C_1(B), C_1(A), and C_2 in harmonic approximation using the known quantum-mechanical result

$$\rho = \prod_{\mathbf{Q}'} (1 - e^{-\hbar\omega_{Q'}/kT})^{-1} \qquad (4)$$

The relative calculated values were similar: 1, 1.05, 0.988, and 0.811 for the structures C_s, C_1(B), C_1(A), and C_2, respectively, which favors our approach.

TABLE 3: Low Vibration Frequencies for Stationary Structures of the 1,2,3-Trifluorobenzene Radical Anion (UB3LYP/6-31+G*)[a]

	vibration mode	
structure	F out-of-plane	pseudorotation
C_s	112.9 (a')	185.1 (a'')
C_1(A)	122.1 (a)	198.7i (a)
C_1(B)	112.3 (a)	181.1 (a)
C_2	201.5 (a)	225.3i (b)

[a] The frequencies are given in units of cm^{-1}.

(iii) Equation 1 assumes a classical character of motion along the pseudorotation coordinate that holds for the case where the value of thermal motion energy kT substantially exceeds the distance between the energy levels of molecule vibrations. Note that the frequencies of vibrations along the pseudorotation coordinate (Table 3) calculated for the C_s and C_1(B) structures are comparable with kT. A more rigorous calculation of the temperature dependence of hfc constants should be performed in the framework of the quantum-mechanical approach.[25] At present, it is difficult to estimate the error of the approximation of the classical nuclei motion used up. However, this approximation is often used to calculate the temperature dependence of hfc constants. In particular, the results obtained within the classical approach for the methyl radical are in fair agreement with experimental data.[26]

4. Conclusions

Results of our ab initio calculations show that the PES of the 1,2,3-trifluorobenzene radical anion is the pseudorotation surface with low energy barriers, which allowed us to expect the manifestations of spectral exchange in the ESR spectra of this radical anion.

The OD ESR method was used to detect the ESR spectrum of the 1,2,3-trifluorobenzene radical anion. The temperature dependence of hfc constants was measured over the range 243−325 K.

The temperature dependence of calculated hfc constants was obtained in the framework of the classical Boltzmann distribution from the UB3LYP/6-31+G* calculated changes in energy and hfc constants during the motion along the pseudorotation gutter. The results of these calculations are in fair agreement with the experimental data.

Acknowledgment. This work was supported by the Russian Foundation for Basic Research (Grant Nos. 04-03-32161 and 04-03-32459) and by the program “Leading Scientific Schools” (Grant No. 84.2003.3).

References and Notes

(1) Schastnev, P. V.; Shchegoleva, L. N. *Molecular Distortions in Ionic and Excited States*; CRC Press: Boca Raton, FL, 1995.

(2) Shteingarts, V. D.; Kobrina, L. S.; Bilkis, I. I.; Starichenko, V. F. *Chemistry of Fluoroarenes. Reaction Mechanisms, Intermediates*; Nauka: Novosibirsk, 1991 (in Russian).

(3) Hasegawa, A.; Shiotani, M.; Hama, Y. *J. Phys. Chem.* **1994**, *98*, 1834.

(4) Hasegawa, A.; Itagaki, Y.; Shiotani, M. *J. Chem. Soc., Perkin Trans.* **1997**, *2*, 1629.

(5) Beregovaya, I. V.; Shchegoleva, L. N. *Int. J. Quantum Chem.* **2002**, *88*, 481.

(6) Vysotsky, V. P.; Salnikov, G. E.; Shchegoleva, L. N. *Int. J. Quantum Chem*. **2004**, *100*, 469.

(7) Vysotsky, V. P.; Shchegoleva, L. N. *J. Struct. Chem.* **2003**, *44*, 946.

(8) Molin, Y. N.; Anisimov, O. A. *Radiat. Phys. Chem.* **1983**, *21*, 77.

(9) Montgomery, J. A., Jr.; Frish, M. A.; Ochterski, J. W.; Petersson, G. A. *J. Chem. Phys*. **1999**, *110*, 2822.

(10) Scott, A. P.; Radom, L. *J. Phys. Chem.* **1996**, *100*, 16502.

(11) Schmidt, M. W.; Baldridge, K. K.; Boatz, J. A.; Elbert, S. T.; Gordon, M. S.; Jensen, H.; Koseki, S.; Matsunaga, N.; Su, K.; Nguyen, S.; Windus, T. L.; Dupuis, M.; Montgomery, J. A. *J. Comput. Chem.* **1993**, *14*, 1347.

(12) Frisch, M. J.; Trucks, G. W.; Schlegel, H. B.; Gill, P. M. W.; Johnson, B. G.; Robb, M. A.; Cheeseman, Keith, J. R. T.; Petersson, G. A.; Montgomery, J. A.; Raghavachari, K.; Al-Laham, M. A.; Zakrzewski, V. G.; Ortiz, J. V.; Foresman, J. B.; Cioslowski, J.; Stefanov, B. B.; Nanayakkara, A.; Challacombe, M.; Peng, C. Y.; Ayala, P. Y.; Chen, W.; Wong, M. W.; Andres, J. L.; Replogle, E. S.; Gomperts, R.; Martin, R. L.; Fox, D. J.; Binkley, J. S.; Defrees, D. J.; Baker, J.; Stewart, J. P.; Head-Gordon, M.; Gonzalez, C.; Pople, J. A. *Gaussian 94*, Revision D.4; Gaussian, Inc.: Pittsburgh, PA, 1995.

(13) Amos, R. D.; Alberts, I. L.; Andrews, J. S.; Colwell, S. M.; Handy, N. C.; Jaytilaka, D.; Kobayashi, P. J.; Koga, N.; Laidig, K. E.; Maslen, P. E.; Murray, C. W.; Rice, J. E.; Sanz, J.; Simandiras, E. D.; Stone, A. J.; Su, M.-D. CADPAC, The Cambridge Analytic Derivatives Package, Issue 6.5, Cambridge, 2001.

(14) MOLDEN, www.cmbi.kun.nl/∼schaft/molden/molden.html.

(15) Molin, Y. N.; Anisimov, O. A.; Melekhov, V. I.; Smirnov, S. N. *Faraday Discuss. Chem. Soc.* **1984**, *78*, 289.

(16) Trifunac, A. D.; Werst, D. W. In *Radical Ionic Systems*; Lund, A., Shiotani, M., Eds.; Kluwer Academic Publishers: Dordrecht, The Netherlands, 1991; p 195.

(17) Duling, D. R. *J. Magn. Reson. B* **1994**, *104*, 105.

(18) Shchegoleva, L. N.; Beregovaya, I. V.; Schastnev, P. V. *Chem. Phys. Lett.* **1999**, *312*, 325.

(19) Hino, S.; Seki, K.; Inokuchi, H. *Chem. Phys. Lett.* **1975**, *36*, 335.

(20) *Energy of Chemical Bonds, Ionization Potentials and Electron Affinities*; Kondratyev, V. N., Ed.; Nauka: Moscow, 1974 (in Russian).

(21) Maier, J. P.; Thommen, F. *Chem. Phys.* **1981**, *57*, 319.

(22) Lozovoy, V. V.; Grigoryants, V. M.; Anisimov, O. A.; Molin, Y. N.; Schastnev, P. V.; Shchegoleva, L. N.; Bilkis, I. I.; Shteingarts, V. D. *Chem. Phys.* **1987**, *112*, 463.

(23) Carrington, A.; McLachlan, A. D. *Introduction to Magnetic Resonance with Application to Chemistry and Chemical Physics*; Harper&Row Publishers: New York, Evanston, and London, 1967.

(24) The program written by A. B. Trofimov and H. Köppel.

(25) Ellinger, Y.; Pauzat, F.; Barone, V.; Douady, J.; Subra, R. *J. Chem. Phys.* **1980**, *72*, 6390.

(26) Tachikava, H.; Igarashi, M.; Ishibashi, T. *Chem. Phys. Lett.* **2002**, *352*, 113.